Journal of Applied Mechanics and Technical Physics, Vol. 43, No. 1, pp. 43–49, 2002

DYNAMICS OF A BUBBLE IN A LIQUID UNDER LASER PULSE ACTION

I. Sh. Akhatov, N. K. Vakhitova, and A. S. Topol'nikov

UDC 533.2

Simulation was performed of the behavior of a vapor bubble in a liquid under laser irradiation in laboratory experiments. A mathematical model was developed to analyze the effect of heat conduction, diffusion, and mass transfer on the bubble dynamics under compression and expansion. It is found that at the stage of collapse, intense condensation occurs on the bubble wall, which results in a significant (more than 15-fold) decrease in bubble mass and an increase in pressure (to 10^5 atm) and temperature (to 10^4 K). Results of numerical calculations of the radius of the first rebound and the amplitude of the divergent shock wave in water are compared with experimental data. It is shown that small (about 1%) additives of an incondensable gas lead to a considerable decrease in mass transfer on the bubble wall.

Introduction. Short-term laser-pulse irradiation of water causes formation of a bubble nucleus in the focal zone, whose further dynamics is determined by heat- and mass-transfer processes. At first, the size of the nucleus increases due to evaporation of the liquid on the bubble wall. Having reached a certain critical radius and cooled to the temperature of the ambient water, the bubble collapses because of the difference between the saturated vapor pressure and atmospheric pressure in the liquid. Compression is accompanied by vapor condensation and an increase in both pressure and temperature inside the bubble. After the collapse, the bubble expands again and performs several damped oscillations. It is found experimentally that the first collapse of the bubble is accompanied by a light flash with a duration of more than 1 nsec [1, 2], and the number of emitted photons is of the order of 10^8 [3]. Simultaneously, a divergent shock wave is formed in water, whose intensity is proportional to the maximum radius of bubble extension [4].

Experimental measurements are greatly hampered by the local pattern and rapidity of the process. Hence, theoretical simulation of this process based on numerical calculations is of primary importance. As has been shown in several recent studies of a similar process — the sonoluminescence of a single gas bubble in a liquid — to adequately describe the behavior of a bubble in a liquid, it is necessary to account for many hydrodynamical aspects, such as the compressibility of a medium, including shock-wave compressibility, heat and mass transfer, diffusion, and chemical reactions with participation of gas components [5–8].

The present paper proposes a mathematical model that describes the dynamics of bubble oscillations in water under laser pulse action. The basis of the model is the assumption of spherical symmetry of the bubble gas and the ambient liquid. This motion is generally described by partial differential equations that express the conservation laws of continuum mechanics taking into account heat conduction and diffusion. The rate of mass transfer on the bubble wall due to vaporization and condensation is determined in accordance with the nonequilibrium Hertz–Knudsen–Langmuir model.

1. Dynamics of a Vapor Bubble. We assume that at the initial time, the bubble is at the point of maximum expansion, the vapor temperature is equal to the temperature of the ambient liquid, and the pressure inside the bubble coincides with the saturated vapor pressure at the given temperature. Since under normal conditions (atmospheric pressure and room temperature) the saturated vapor pressure (roughly 0.02 atm) is well below the water pressure, the bubble begins to collapse.

Institute of Mechanics, Ufa Scientific Center, Russian Academy of Sciences, Ufa 450000. Translated from Prikladnaya Mekhanika i Tekhnicheskaya Fizika, Vol. 43, No. 1, pp. 52–59, January–February, 2002. Original article submitted May 22, 2001.

0021-8944/02/4301-0043 $27.00

To simulate the problem, the entire spatial region is divided into three subregions along the radial coordinate according to the algorithm proposed in [9, 10]: subregion 1 [$0 \leqslant r \leqslant a(t)$] occupied by vapor [$a(t)$ is the bubble radius], subregion 2 [$a(t) < r \leqslant R(t)$] occupied by water and bounded by a certain, intentionally introduced Lagrangian boundary, and subregion 3 [$R(t) < r < \infty$] filled with a poorly compressible liquid. The $R(t)$ is chosen such that during the entire cycle of bubble oscillations, the rate of change of $\dot{R}(t)$ remains low compared to the speed of sound in water. In this case, the law of variation of $R(t)$ is defined by an equation similar to the Rayleigh–Plesset equation. In the present paper, we set $R_0 = 1.5a_0$ (a_0 is the initial bubble radius).

To describe the parameters of the vapor inside the bubble for $r \leqslant a(t)$ and those of the water in the region $a(t) \leqslant r \leqslant R(t)$ adjoining the bubble surface, we consider the system of partial differential equations taking into account heat conduction in the spherical symmetry approximation:

$$\frac{\partial \rho}{\partial t} + \frac{1}{r^2}\frac{\partial}{\partial r}(\rho u r^2) = 0, \qquad \frac{\partial}{\partial t}(\rho u) + \frac{1}{r^2}\frac{\partial}{\partial r}(\rho u^2 r^2) + \frac{\partial p}{\partial r} = 0; \tag{1}$$

$$\frac{\partial e}{\partial t} + \frac{1}{r^2}\frac{\partial}{\partial r}\Big(u r^2 (e+p) - \lambda r^2 \frac{\partial T}{\partial r}\Big) = 0. \tag{2}$$

Here ρ, u, p, T, and e are the density, rate, pressure, temperature, and specific total energy per unit volume, respectively, and λ is the thermal conductivity.

System (1), (2) is closed by the equations of state for the vapor and water. In the present paper, for the vapor, we used the Van der Waals relation

$$p_{\rm v} = \frac{\rho_{\rm v} B_{\rm v} T_{\rm v}}{1 - b_1 \rho_{\rm v}} - b_2 \rho_{\rm v}^2, \qquad \varepsilon_{\rm v} = \frac{e_{\rm v}}{\rho_{\rm v}} - \frac{u_{\rm v}^2}{2} = \frac{B_{\rm v} T_{\rm v}}{\gamma - 1} - b_2 \rho_{\rm v}, \tag{3}$$

where $B_{\rm v} = 458.9$ J/(kg·K), $b_1 = 1.694 \cdot 10^{-3}$ m^3/kg, $b_2 = 1708.6$ J·m^3/kg^2, and $\gamma = 1.3$.

To describe the parameters of the water, we use the Mie–Grüneisen equation of state, which provides for good agreement between calculation results and experimental data for the region of strong compression and moderate expansion [10]:

$$p_l = p_c(\rho_l) + \Gamma(\rho_l) c_{\rm v} \rho_l T_l, \qquad \varepsilon_l = e_l/\rho_l - u_l^2/2 = \varepsilon_c(\rho_l) + c_{\rm v} T_l.$$

Here

$$p_c(\rho_l) = A\Big(\frac{\rho_l}{\rho_{l0}}\Big)^{2/3} \exp\Big(b\Big[1 - \Big(\frac{\rho_l}{\rho_{l0}}\Big)^{-1/3}\Big]\Big) - K\Big(\frac{\rho_l}{\rho_{l0}}\Big)^{4/3},$$

$$\varepsilon_c(\rho_l) = \frac{3A}{\rho_{l0} b} \exp\Big(b\Big[1 - \Big(\frac{\rho_l}{\rho_{l0}}\Big)^{-1/3}\Big]\Big) - \frac{3K}{\rho_{l0}}\Big(\frac{\rho_l}{\rho_{l0}}\Big)^{1/3},$$

the values $A = 3.492 \cdot 10^8$ Pa, $K = 8.283 \cdot 10^8$ Pa, $b = 16.0558$, $c_{\rm v} = 3270$ J/(kg·K), and $\rho_{l0} = 998$ kg/m^3 are chosen so as to provide for a best fit to experimental data, and $\Gamma(\rho_l)$ is the Grüneisen coefficient specified as an analytical function of density.

Boundary conditions for the bubble surface are formulated with allowance for vaporization and condensation that occur there. Equating heat fluxes, we obtain the equation relating the temperature gradients for the vapor and water:

$$\lambda_l \frac{\partial T_l}{\partial r}\Big|_{r=a} - \lambda_{\rm v} \frac{\partial T_{\rm v}}{\partial r}\Big|_{r=a} = jl(p_{\rm v}|_{r=a}).$$

Here l is the specific heat of vaporization and j is the phase-transfer rate during vaporization and condensation:

$$j = (\alpha/\sqrt{2\pi B_{\rm v}})(p_S(T_l|_{r=a})/\sqrt{T_l|_{r=a}} - \Gamma_{\rm v} p_{\rm v}|_{r=a}/\sqrt{T_{\rm v}|_{r=a}}\,), \tag{4}$$

which is expressed by the generalized Hertz–Knudsen–Langmuir equality taking into account the corrections for the mobility of the interface [11]:

$$\Gamma_{\rm v} = \exp(-\Omega^2) - \Omega\sqrt{\pi}\left(1 - \frac{2}{\sqrt{\pi}}\int_0^{\Omega} \exp(-x^2)\,dx\right), \quad \Omega = \frac{j\sqrt{B_{\rm v} T_{\rm v}|_{r=a}}}{\sqrt{2} p_{\rm v}|_{r=a}} = -\frac{u_{\rm v}|_{r=a} - \dot{a}}{\sqrt{2 B_{\rm v} T_{\rm v}|_{r=a}}}.$$

Generally, we introduce a temperature jump on the bubble wall:

$$[T] = T_l|_{r=a} - T_{\rm v}|_{r=a} = 0.45 j T_S/(\sqrt{2 B_{\rm v} T_S}\,\rho_{\rm v}|_{r=a}).$$

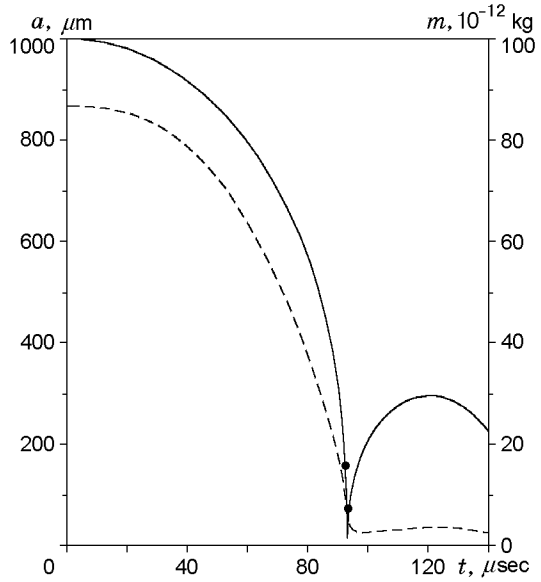

Fig. 1

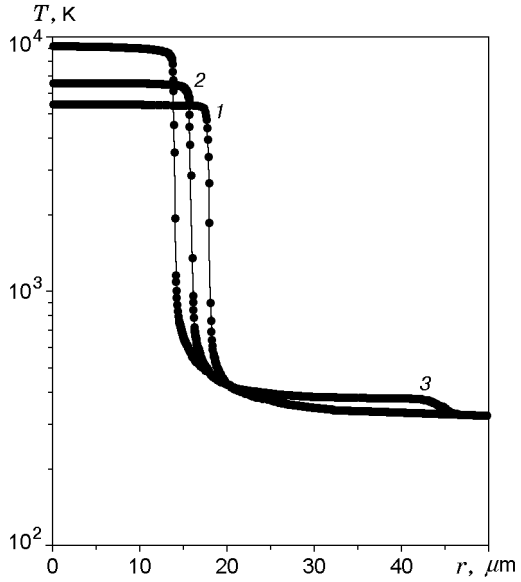

Fig. 2

Fig. 1. Bubble radius (solid curve) and vapor mass (dashed curve) versus time at $a_0 = 1$ mm and $\alpha = 0.075$ (the points refer to the moments of transition from the slow stage to the rapid stage and vice versa).

Fig. 2. Spatial distributions of temperature near collapse for $a_0 = 1$ mm and $\alpha = 0.075$ and $t = -4.76$ (1), 0.45 (2), and 7.22 nsec (3); the points correspond to the temperature in the calculation cells.

For $r = a(t)$, the velocities and pressures of the vapor and liquid are related by

$$u_{\rm v}|_{r=a} = \dot a - j/\rho_{\rm v}|_{r=a}, \qquad u_l|_{r=a} = \dot a - j/\rho_l|_{r=a},$$

$$p_{\rm v}|_{r=a} = p_l|_{r=a} + 2\sigma/a + 4\mu_l u_l|_{r=a}/a = p_l|_{r=a} + 2\sigma/a + (4\mu_l/a)(\dot a - j/\rho_l),$$

where σ and μ_l are the surface tension and dynamic viscosity of the water, respectively.

The variation of the external radius of the compressed liquid region $R(t)$ is expressed by the generalized Rayleigh–Plesset equality [12]

$$\Big(1 - \frac{\dot R}{C_l}\Big) R\ddot R + \frac{3}{2}\Big(1 - \frac{\dot R}{3C_l}\Big)\dot R^2 = \Big(1 + \frac{\dot R}{C_l}\Big)\frac{p_l|_{r=R} - p_{l0}}{\rho_{l0}} + \frac{R}{\rho_{l0}C_l}\frac{d}{dt}\Big(p_l|_{r=R} - p_{l0}\Big), \tag{5}$$

where $C_l = 1500$ m/sec is the speed of sound in water and $p_{l0} = 1$ atm is the initial pressure in the liquid.

In the present paper, values of the thermodynamic coefficients for the vapor and water ($\lambda_{\rm v}$, λ_l, μ_l, σ, p_S, and l) are approximated by analytical formulas based on well-known tabular data [13].

Numerical integration of the system of differential equations (1) and (2) in the region $0 \leqslant r \leqslant R(t)$ for the entire period of bubble oscillations is too tedious and time-consuming. Therefore, at the slow stage of the process, which is characterized by low Mach numbers, a homobaric approximation for vapor and the incompressibility condition for the water are used instead of equalities (1) and (2) [14]. As a result, the full system of differential equations is solved only for a narrow time interval in which the compression–extension bubble rate is comparable to the speed of sound in vapor.

Calculations for the homobaric model are performed using an implicit finite-difference scheme of second-order approximation, and the Rayleigh–Plesset equation (5) is solved by the Runge–Kutta method of fifth-order accuracy. The full system of Eqs. (1) and (2) is solved numerically using Godunov's scheme.

Figures 1 and 2 show results of numerical calculations of the collapse of a vapor bubble with $a_0 = 1$ mm. At the initial moment, the vapor inside the bubble is in the saturation state at the specified liquid temperature $T_{l0} = 296$ K. Figure 1 shows curves of bubble radius and vapor mass m versus time. The points refer to the moments of conversion from calculations by simplified models describing the medium (the homobaric model for the vapor and the model of an incompressible liquid for the water) to calculations by the full model and vice versa.

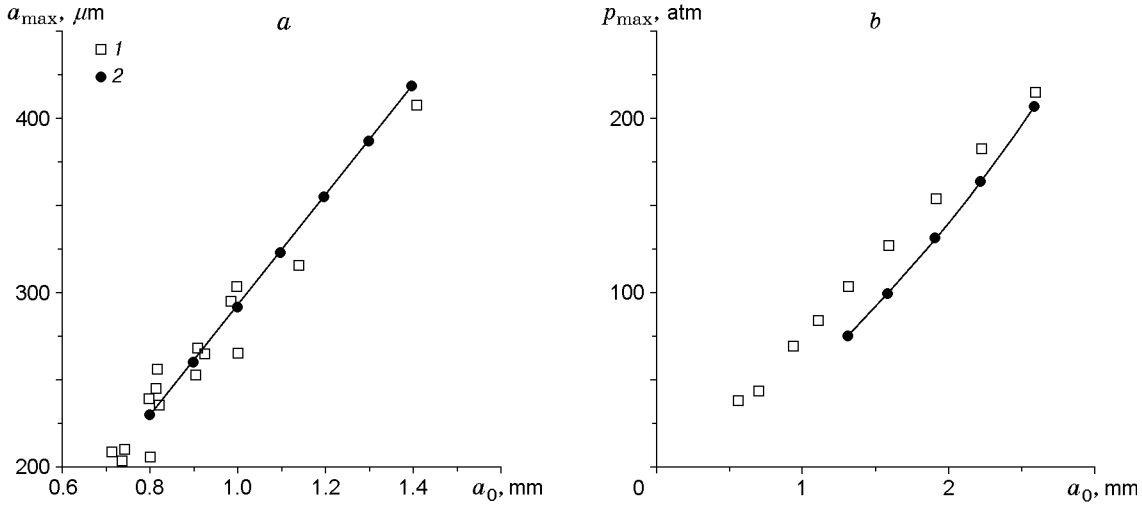

Fig. 3. Maximum first rebound radius (a) and shock-wave amplitude in the water at a distance of 3 mm from the center of the bubble (b) versus initial bubble radius: points 1 are experimental results and points 2 are calculated values.

During collapse, the minimum bubble radius is 14 μm and the vapor mass is roughly 6% of the initial value. The latter is accounted for by vapor condensation on the bubble wall during collapse; the condensation rate is given by Eq. (4). The accommodation coefficient α in (4) such that the calculation results fit the experimental data. In this paper, this coefficient is equal to 0.075 and is determined from the experimental values of the first rebound for initial bubble radius $a_0 = 1$ mm.

We note that because of condensation at the stage of compression, the bubble pressure grows not so rapidly as in the case of a gas bubble with a constant mass. As a result, a deeper collapse is possible, and, consequently, much higher pressure and temperature can be reached inside the bubble.

Figure 2 shows temperature distributions along the radius in the vapor and liquid for three sequential moments close to the moment when the radius reached its minimum value. During collapse, the gas inside the bubble is heated almost uniformly, except in a thin boundary layer near the surface, where the temperature decreases abruptly to the water temperature. This results in a decrease in the probability of formation of a convergent shock wave in the bubble because any nonlinear excitation on the surface, propagating toward the center of the bubble, reaches the region with increasing speed of sound and then degenerates to a weakly acoustic excitation. The calculation results show that during expansion, the bubble generates a shock wave in the water (curve 3 in Fig. 2). The maximum vapor pressure and temperature in the center of the bubble are 10^5 atm and 10^4 K, respectively.

The calculation results presented in this paper were compared to the experimental data of [4, 15]. Figure 3 show curves of the maximum bubble radius during the first rebound and the amplitude of the divergent shock wave in the water (at a distance of 3 mm from the center of the bubble) versus initial bubble size.

2. Effect of Incondensable Gas Additives. Under experimental conditions, the bubble generated by a laser pulse contains not only water vapor but also additives of other gases. These gases can result from recombination of plasma after laser beam focusing, chemical reactions inside the bubble or diffusion from the ambient liquid. To estimate the effect of the incondensable gas on the dynamics of a vapor cavity, we consider the model of a two-component vapor–gas medium inside the bubble.

In this case, Eqs. (1) describe the laws of conservation of mass and momentum for the entire mixture. With allowance for diffusive additives, the energy equation is written as

$$\frac{\partial e}{\partial t} + \frac{1}{r^2}\frac{\partial}{\partial r}\left(ur^2(e+p)\right) = \frac{1}{r^2}\frac{\partial}{\partial r}\left(\lambda r^2 \frac{\partial T}{\partial r}\right) + \frac{1}{r^2}\frac{\partial}{\partial r}\left(\rho r^2 D \frac{\partial k}{\partial r}\left(i_{\mathrm{v}} - i_{\mathrm{g}}\right)\right),$$

where k and D are the vapor mass fraction and the binary diffusion coefficient for this mixture, respectively, $i = \varepsilon + p/\rho$ is the enthalpy, and the subscripts "v" and "g" refer to the parameters of the vapor and gas, respectively.

To calculate k, we write the equation of binary diffusion in the form

$$\frac{\partial k}{\partial t} + u\,\frac{\partial k}{\partial r} = \frac{1}{\rho r^2}\,\frac{\partial}{\partial r}\Big(\rho r^2 D\,\frac{\partial k}{\partial r}\Big).$$

The relationship between the parameters of the individual components and the entire mixture is specified by the following equalities: $\rho_{\rm v} = k\rho$, $\rho_{\rm g} = (1-k)\rho$, $u = ku_{\rm v} + (1-k)u_{\rm g}$, $p = p_{\rm v} + p_{\rm g}$, $\varepsilon = k\varepsilon_{\rm v} + (1-k)\varepsilon_{\rm g}$, $\rho_{\rm v}(u-u_{\rm v}) = -\rho_{\rm g}(u-u_{\rm g}) = \rho D\,\partial k/\partial r$, and $T = T_{\rm v} = T_{\rm g}$.

As the incondensable gas, we consider air. We write the equation of state for air, as for water vapor, in the form of the van der Waals dependence (3), in which we set $B_{\rm g} = 284.75$ J/(kg·K), $b_{1g} = 1.294\cdot 10^{-3}$ m^3/kg, $b_{2g} = 166.7$ J·m^3/kg^2, and $\gamma_{\rm g} = 1.4$. The binary diffusion coefficient for water vapor in air is defined as a function of temperature: $D = 2.16\cdot 10^{-5}(T/273)^{1.8}$.

The mass fraction of the vapor–gas mixture components can vary during bubble oscillations not only due to vaporization or condensation but also due to diffusion of the gas from the liquid through the bubble wall.

We consider the diffusion equation for air in water in the form

$$\frac{\partial c}{\partial t} + \frac{a^2\dot a}{r^2}\,\frac{\partial c}{\partial r} = \frac{D_l}{r^2}\,\frac{\partial}{\partial r}\Big(r^2\,\frac{\partial c}{\partial r}\Big) \tag{6}$$

with the boundary conditions

$$c|_{r=\infty} = c_\infty, \qquad c|_{r=a(t)} = c_a(t),$$

where c is the gas mass fraction and D_l is the diffusion coefficient.

The solution of Eq. (6) can be approximately written as

$$c(r,t) = c_\infty + (c_a(t) - c_\infty)\exp\left(-(r-a(t))/\delta(t)\right), \tag{7}$$

where δ is the effective thickness of the diffusion layer near the bubble surface. Substituting (7) into (6), we obtain the following estimate for the increase in gas mass inside the bubble:

$$\Delta m_{\rm g} \approx 4\sqrt{2D_l\Delta t}\,\pi a_{\max}^2 c_\infty \rho_{l0},$$

where Δt is the time of bubble oscillations. For the following characteristic values of the parameters: $D_l \approx 10^{-9}$ m^2/sec, $\Delta t \approx 10^{-4}$ sec, $a_{\max} \approx 10^{-3}$ m, and $c_\infty \approx 10^{-5}$, we have $\Delta m_{\rm g} \approx 5\cdot 10^{-14}$ kg, which is 3 or 4 orders of magnitude smaller than the value of the initial bubble mass (see Fig. 1).

Thus, the estimate of the intensity of gas diffusion from the water into the bubble shows that this process does not have a significant effect on the solution during one period of bubble oscillations. This is supported by experimental measurements, which show that the light pulse intensity — one of the principal characteristics of the process — does not depend on the sort and mass of the gas dissolved in the water [2]. Therefore, in the present work, we assume that air diffusion through the bubble wall is absent.

Numerical calculations of the problem for a two-component gas mixture were performed for initial gas concentrations of the order of 1%. The remaining parameters were the same as those for a vapor bubble. Calculations for collapse of a bubble with $a_0 = 1$ mm and $k_0 = 0.99$ yielded the following values of the principal characteristics: a minimum radius of 16.5 μm, a first rebound radius of 360 μm, and a collapsing bubble mass of $8\cdot 10^{-12}$ kg. Comparison of these results with the values obtained for a vapor bubble (14 μm, 290 μm, and $5.5\cdot 10^{-12}$ kg, respectively) shows that addition of a small amount of gas leads to considerable changes in the solution.

To explain the effect observed, we consider the spatial distribution of vapor concentration at the stage of bubble compression. Figure 4 shows that the vapor concentration is uniform ($k = 0.99$) virtually over the entire region occupied by the bubble, except in a small neighborhood near the bubble wall, where the gas concentration decreases abruptly (by 30–40%). As a result of such distribution, a thin boundary layer with a high gas content forms near the interface, which leads to a significant decrease in mass transfer. Figure 5 shows curves of rebound radius and maximum temperature of the mixture at the center of the bubble versus initial gas concentration. An increase in initial gas concentration from 0 to 10% leads to an increase in $a_{\max}$ from 290 to 620 μm and to a corresponding decrease in the peak temperature from 10^4 to $5.2\cdot 10^3$ K.

Conclusions. A mathematical model is proposed that describes spherically symmetric motion of a bubble in a liquid taking into account heat and mass transfer for a two-component gas mixture.

The laser-induced collapse of a spherical vapor cavity in water is numerically calculated on the basis of the model proposed. It is shown that the dynamics of the bubble is largely determined by vaporization and condensation

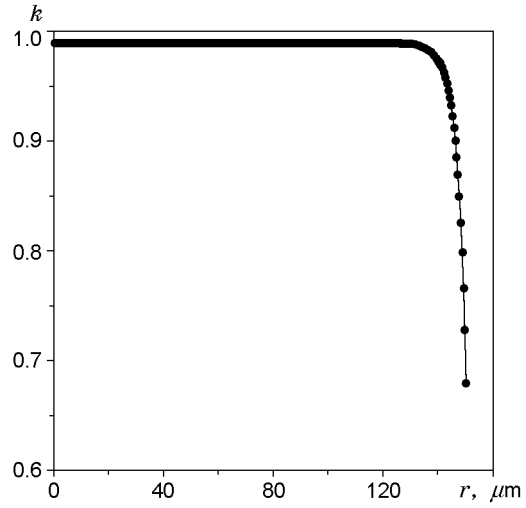

Fig. 4

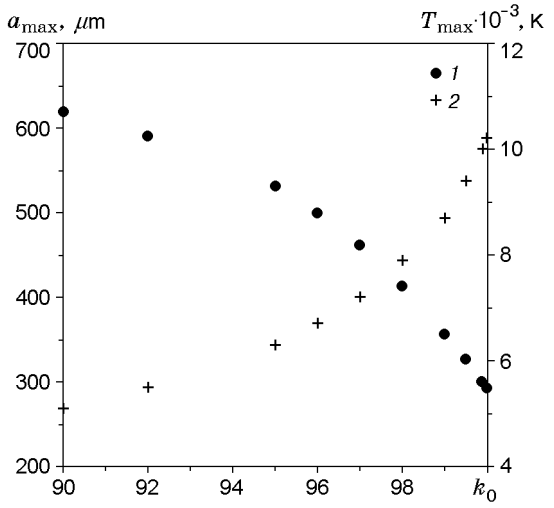

Fig. 5

Fig. 4. Vapor concentration distribution over the radius inside the bubble at the stage of compression ($t = -530$ nsec with respect to the collapse time) for $a_0 = 1$ mm, $\alpha = 0.075$, and $k_0 = 0.99$ (the points are values of the concentration in calculation cells).

Fig. 5. Rebound radius (1) and maximum temperature inside the bubble (2) versus initial vapor concentration for $a_0 = 1$ mm and $\alpha = 0.075$.

processes on its wall. Because of a decrease in vapor mass during bubble compression, high pressure and temperature are reached inside the bubble, which causes bubble luminescence. Results of the numerical calculations are in good agreement with experimental data.

The investigation performed shows that gas diffusion from the ambient liquid has virtually no effect on the dynamics of the vapor cavity. However, the presence of even small amounts of gas inside the bubble (about 1% of the vapor mass) leads to considerable weakening of collapse.

The authors thank R. I. Nigmatulin and R. Kh. Bolotnova for helpful discussions.

This work was supported by the Ministry of Science and Engineering of Germany (Contract No. RUS-133-97), European Commission [INCO COPERNICUS IC15-CT98-0141 (DG 12-MZCN)], and the Ministry of Atomic Energy of the Russian Federation (Grant No. 6.25.19.19.99.806).

REFERENCES

1. A. A. Buzukov and V. S. Teslenko, "Sonoluminescence upon focusing of laser radiation into liquid," *Pis'ma Zh. Tekh. Fiz.*, **14**, No. 5, 286–289 (1971).
2. O. Baghdassarian, B. Tabbert, and G. A. Williams, "Luminescence characteristics of laser-induced bubbles in water," *Phys. Rev. Lett.*, **83**, No. 12, 2437–2440 (1999).
3. C. D. Ohl, O. Lindau, and W. Lauterborn, "Luminescence from spherically and aspherically collapsing laser induced bubbles," *Phys. Rev. Lett.*, **80**, No. 2, 393–396 (1998).
4. O. Lindau and W. Lauterborn, "Laser-produced cavitation — studied with 100 million frames per second," in: *Nonlinear Acoustics at the Turn of Millennium*, Proc. AIP Conf. (Göttingen, Germany, Sept. 1–4, 1999), Vol. 524, Amer. Inst. of Phys., Melville–New York (2000), pp. 385–388.
5. V. Q. Vuong and A. J. Szeri, "Sonoluminescence and diffusive transport," *Phys. Fluids*, **8**, No. 9, 2354–2364 (1996).
6. K. Yasui, "Alternative model of single-bubble sonoluminescence," *Phys. Rev. E*, **56**, No. 6, 6750–6760 (1997).
7. W. C. Moss, D. A. Young, J. A. Harte, et al., "Computed optical emissions from a sonoluminescing bubble," *Phys. Rev. E*, **59**, No. 3, 2986–2992 (1999).
8. B. D. Storey and A. J. Szeri, "Water vapor, sonoluminescence and sonochemistry," *Proc. Roy. Soc. London, Ser. A*, **456**, 1685–1709 (2000).

9. R. I. Nigmatulin, I. Sh. Akhatov, N. K. Vakhitova, and A. S. Topolnikov, "Bubble collapse and shock wave formation in sonoluminescence," in: *Nonlinear Acoustics at the Turn of Millennium*, Proc. AIP Conf. (Göttingen, Germany, Sept. 1–4, 1999), Vol. 524, Amer. Inst. of Phys., Melville–New York (2000), pp. 433–436.
10. R. I. Nigmatulin, I. Sh. Akhatov, N. K. Vakhitova, et al., "Mathematical modeling of a single bubble and multibubble dynamics in a liquid," in: *Proc. of the Int. Conf. on Multiphase Systems* (Ufa, June 15–17, 2000), Gilem Publ. and Pol Publ., Ufa (2000), pp. 294–301.
11. R. W. Schrage, *A Theoretical Study of Interphase Mass Transfer*, Columbia Univ. Press, New York (1953).
12. R. I. Nigmatulin, I. Sh. Akhatov, and N. K. Vakhitova, "Forced oscillations of a gas bubble in a spherical volume of a compressed liquid," *Prikl. Mekh. Tekh. Fiz.*, **40**, No. 2, 111–118 (1999).
13. S. L. Rivkin and A. A. Aleksandrov, *Thermal-Physics Characteristics of Water and Water Vapor* [in Russian], Énergiya, Moscow (1980).
14. R. I. Nigmatulin, *Dynamics of Multiphase Media*, Parts 1 and 2, Hemisphere, New York (1991).
15. C. D. Ohl, T. Kurz, R. Geisler, et al., "Bubble dynamics, shock waves and sonoluminescence," *Philos. Trans. Roy. Soc. London, Ser. A*, **357**, 269–294 (1999).